Published in final edited form as:
Estuaries Coast. 2018 May 1; 41(3): 690–707. doi:10.1007/s12237-017-0328-9.

Seasonal oxygen dynamics in a warm temperate estuary: effects of hydrologic variability on measurements of primary production, respiration, and net metabolism

Michael C. Murrell[1,*], **Jane M. Caffrey**[2], **Dragoslav T. Marcovich**[1], **Marcus W. Beck**[1], **Brandon M. Jarvis**[1], and **James D. Hagy III**[1]

[1]US Environmental Protection Agency, Gulf Ecology Division, 1 Sabine Island Dr., Gulf Breeze, FL 32561, USA

[2]Center for Diagnostics and Bioremediation, University of West Florida, 11000 University Parkway, Pensacola, FL, 32514, USA

Abstract

Seasonal responses in estuarine metabolism (primary production, respiration, and net metabolism) were examined using two complementary approaches. Total ecosystem metabolism rates were calculated from dissolved oxygen time series using Odum's open water method. Water column rates were calculated from oxygen-based bottle experiments. The study was conducted over a spring-summer season in the Pensacola Bay estuary at a shallow seagrass-dominated site and a deeper bare-bottomed site. Water column integrated gross production rates more than doubled (58.7 to 130.9 mmol O_2 m^{-2} d^{-1}) from spring to summer, coinciding with a sharp increase in water column chlorophyll-a, and a decrease in surface salinity. As expected, ecosystem gross production rates were consistently higher than water column rates, but showed a different spring-summer pattern, decreasing at the shoal site from 197 to 168 mmol O_2 m^{-2} d^{-1} and sharply increasing at the channel site from 93.4 to 197.4 mmol O_2 m^{-2} d^{-1}. The consistency among approaches was evaluated by calculating residual metabolism rates (ecosystem - water column). At the shoal site, residual gross production rates decreased from spring to summer from 176.8 to 99.1 mmol O_2 m^{-2} d^{-1}, but were generally consistent with expectations for seagrass environments, indicating that the open water method captured both water column and benthic processes. However, at the channel site, where benthic production was strongly light-limited, residual gross production varied from 15.7 mmol O_2 m^{-2} d^{-1} in spring to 86.7 mmol O_2 m^{-2} d^{-1} in summer. The summer rates were much higher than could be realistically attributed to benthic processes, and likely reflected a violation of the open water method due to water column stratification. While the use of sensors for estimating complex ecosystem processes holds promise for coastal monitoring programs, careful attention to the sampling design, and to the underlying assumptions of the methods, is critical for correctly interpreting the results. This study demonstrated how using a combination of approaches yielded a fuller understanding of the ecosystem response to hydrologic and seasonal variability.

[*]Corresponding Author: Phone: 850-934-2433, Fax: 850-934-2401, murrell.michael@epa.gov.

Keywords

Primary Production; Plankton Community Respiration; Net Ecosystem Metabolism; Dissolved Oxygen; Estuary

Introduction

Estuaries are biogeochemically dynamic ecosystems receiving and rapidly processing organic matter and nutrients delivered from the landscape and the adjacent seaward boundary. The complex spatial and temporal variation in the delivery of allochthonous materials to an estuary, in turn, affects primary production (GPP), community respiration (CR), and net ecosystem metabolism (NEM = GPP-CR). While estuarine and coastal ecosystems represent a small proportion of global surface area, understanding their productivity and the magnitudes of carbon fluxes is necessary for constraining global budgets (Smith and Hollibaugh 1993, Cai 2011)

Estuaries provide numerous ecosystem services for humans, including fish and shellfish harvesting, recreation, transportation, waste disposal, and other commercial activities (Costanza et al. 1997). One common consequence of human activities is to increase nutrient loading to coastal environments, from point and non-point sources. Excess nutrients can strongly stimulate aquatic primary production (i.e., eutrophication) altering the metabolic balance between primary production and respiration. Thus, eutrophication can alter net carbon balance in coastal environments, the net exchange of atmospheric CO2, and the quality of food resources available for estuarine consumers (Kemp and Testa 2011). Eutrophication can also strongly impact O_2 dynamics, typically causing increased variability on short time scales with periods of strong supersaturation and depletion (i.e., hypoxia).

Measures of primary production, respiration, and net ecosystem metabolism provide fundamental information about the trophic state of aquatic ecosystems, which in turn can be useful for local resource managers in making land-use decisions. However, in practice, measures of aquatic metabolism are logistically difficult to carry out and to scale appropriately, owing to the high spatial and temporal variability of estuarine environments. Furthermore, results may be strongly method-dependent, making it difficult to compare measurements across different studies, different systems, or different periods of time (Cloern et al. 2014). Key environmental factors that influence rates of ecosystem production and respiration include light and water clarity, temperature, nutrient and organic matter loading, water residence time, and water depth (Kemp and Testa 2011).

The oxygen-based open water method pioneered by Odum (1956) quantifies the diel oscillations in dissolved O_2 concentrations to estimate daily integrated gross production, respiration and net metabolism, and is one of a family of incubation-free methods used to estimate ecosystem processes (e.g., see Williams et al. 2013). Originally developed for streams, Odum's approach has been subsequently applied to various aquatic ecosystems, including lakes (e.g., Staehr et al. 2007, Coloso et al. 2008, Tonetta et al. 2016), estuaries (e.g., Swaney et al. 1999, Caffrey 2004, Caffrey et al. 2014, Nidzieko et al. 2014), and coastal embayments (Champenois and Borges 2012). Recent reviews have provided useful

discussions of the theory, the governing equations, and the assumptions and limitations of the method (Staehr et al. 2010, Needoba et al. 2012). Reduced cost and improvements in control of biofouling on *in situ* datasondes have the potential to greatly increase application of this method. Alternatively, component measurements isolating either water samples in bottles or the benthos in benthic chambers or cores can provide insight into the factors driving water column or benthic production and respiration. While several previous studies have analyzed long-term dissolved O_2 time series (Caffrey 2004, Caffrey et al. 2014, Beck et al. 2015), few estuarine studies that have sought to compare open water estimates with alternative methods (e.g., Ziegler and Benner 1998). In this study we used open water and bottle incubation methods to measure primary production, respiration and net ecosystem metabolism in the Pensacola Bay estuary at two contrasting locations: a shallow seagrass habitat and an adjoining deeper area. This design allowed us to evaluate how these distinctive habitats responded to seasonal variability in hydrology, and provided insight into the assumptions and limitations of each method.

Study site

Pensacola Bay is a shallow, river-dominated estuary located in the northeastern Gulf of Mexico (Fig. 1). Freshwater is delivered via the Escambia, Yellow, and Blackwater Rivers, contributing 71%, 26% and 4% of the total gaged flow, respectively (Thorpe et al. 1997). It has moderate to high phytoplankton productivity (~290 g C m^{-2} y^{-1}, Murrell et al. 2007) compared to other estuarine and coastal systems (Cloern et al. 2014). The seasonal river flow pattern creates stratification in the mesohaline region of Pensacola Bay, particularly during spring and summer, contributing to depletion of dissolved O_2 in bottom waters (USEPA 2005, Hagy and Murrell 2007). Stratification tends to dissipate in the lower portion of Pensacola Bay, which rarely experiences hypoxia (Hagy and Murrell 2007). Compared to nearby estuaries such as Mobile Bay, suspended particulate concentrations are relatively low contributing to high water transparency, such that approximately half of the bay bottom is euphotic (Murrell et al. 2009). Seagrasses cover 14.3 km^2 (3 % of the bottom), however this coverage is only 37 % of a 1960 coverge of 38.6 km^2 (8 % of the bottom), suggesting a significant decline in seagrasses over the past ~60 years (Handley et al. 2007, Yarbro and Carlson 2013). Relatively seagrass healthy beds of *Thalassia testudinum* and *Halodule beaudettei* (formerly *Halodule wrightii*) remain in lower Pensacola Bay and Santa Rosa Sound.

The study was located in lower Pensacola Bay near its confluence with Santa Rosa Sound (30.36°N, 87.20°W, Fig. 1) in a region with fringing seagrass beds graduating to deeper unvegetated habitat comprised of sand-silt sediments. Two sites were sampled across this depth gradient: a seagrass dominated site (1.5 m water depth) and a nearby un-vegetated channel site (~0.5 km away, 6 m of water depth). Thus, both sites were expected to experience similar hydrologic variability, but exhibit different partitioning and seasonal dynamics of primary production and community respiration.

Methods

Continuous monitoring

Water quality time series were collected from April to September 2013 using Wetlabs® WQM instruments (Philomath, Oregon) deployed at each site, logging temperature, salinity, depth, dissolved O_2, turbidity, chlorophyll *a* (Chl-*a*) fluorescence, and fluorescent dissolved organic matter (FDOM) at 30 minute intervals. At the channel site, the instrument was mounted on a surface buoy in the top 1 m of the water column. At the shoal site, the instrument was fixed to a piling 0.5 m above the bottom, corresponding to approximately 1 m below the surface. The instruments were outfitted with extensive anti-fouling technology provided by the manufacturer (copper housing and copper wire mesh at the water inlet, bleach injection system), which allowed for prolonged deployments (~ 12 weeks) without loss of data quality. Two deployments were required at each site, with a data gap from 2–10 July 2013 occurring when the instruments were being serviced. Inspection of pre- and post-calibration reports from the manufacturer indicated that sensors stability was excellent. In particular, O_2 sensor calibrations showed very small drift pre- and post-deployment (~ 1–5%), thus corrections were not attempted nor considered necessary.

A weather station (Endeco/YSI®) was deployed at the US Environmental Protection Agency laboratory dock within 5 km of the study sites to monitor wind speed, wind direction, air temperature, barometric pressure, relative humidity, and solar irradiance. The anemometer was fixed at a height of 5.75 m above the water surface and normalized to 10 m (U_{10}) using the seventh root law (Ro and Hunt 2006). Solar radiation (~400–1100 nm, W m^{-2}) was measured with a LI-COR LI-200SA pyranometer. The weather time series included several brief data gaps (maximum gap = 20 h) that were repopulated with climatological means by hour calculated from adjacent time periods within the same month.

Field sampling

The shoal (seagrass dominated) and channel sites were visited in the early morning (~6 am local time) at weekly to bi-weekly intervals. Water column profiles of temperature, salinity, dissolved O_2, turbidity, FDOM, Chl-*a* fluorescence and photosynthetically active radiation (PAR) were measured using a Seabird SBE25 CTD system. Although PAR profiles were obtained with the CTD, the low sun angle in early morning caused inconsistent measures of light attenuation. Thus, Secchi disk depth from the channel site was used to calculate light attenuation.

Surface water was collected (~0.5 m under surface) using a low-pressure submersible, centrifugal bilge pump (rule.industries.com). The pump outlet, mated with 1.8 cm (ID) Tygon® tubing, produced a smooth bubble-free flow at a rate of ~15 L min^{-1}. Visual inspection of pump-collected water samples revealed that plankton were intact and viable. In addition to the smaller phytoplankton, live zooplankton were routinely observed in pumped samples, including adult and larval copepods, small hydroids, ctenophores, larvaceans, and veliger larvae, ranging in size from <100 μm to >1000 μm in length. Prior experience with a similar pump system demonstrated that it was suitable for dissolved gas sampling; a pairwise comparison of dissolved O_2 measurements in pump-collected vs. in situ sensor

showed excellent agreement (O_2 pump (mg L^{-1}) = 0.96 * O_2 in situ + 0.33, R^2 = 0.94, n = 142, Murrell unpublished data). Between sampling dates, the pump and tubing system was flushed with deionized water and fully drained for storage.

Water samples for dissolved and particulate constituents were collected in opaque HDPE bottles and processed upon return to the laboratory (within 1 h). For nutrients (NH_4^+, NO_2^-, NO_3^-, PO_4^{3-}, and SiO_3^{2-}), water was passed through GF/F filters and the filtrate was frozen (−70 °C) until analysis within 6 months. Ammonium was analyzed using a fluorometric method (Holmes et al. 1999); other nutrients were analyzed using either a Thermo Fisher Aquakem 200 discrete analyzer or an Astoria-Pacific continuous flow analyzer using standard colorimetric methods (APHA 2005). For Chl-*a*, water (100 to 600 ml) was filtered onto GF/F filters and frozen (−70 °C) until analysis within 3 months. Chl-*a* was extracted from the filters using buffered methanol aided by sonication and analyzed fluorometrically (Welschmeyer 1994). The extracted Chl-*a* data were used to calibrate fluorescence sensors on the CTD and the WQM instruments by fitting to paired measurements using reduced-major axis (Model II) regression analysis (Sokal and Rohlf 1995). For bottle experiments, water was pumped directly into a series of 20 –24 300 ml BOD bottles using a 4-place fork-shaped manifold, constructed of 1.2 cm (ID) household CPVC tubing. The spacing of fork tines matched the BOD bottle openings when arranged in wire racks. Water was allowed to overflow the bottles by 1–2 volumes, which rinsed the bottles and purged atmospheric O_2, then capped and stored in the dark at ambient temperature until return to the lab (within 1 h).

Water column Production-Respiration Experiments

In the lab, four bottles were immediately fixed with Winkler reagents (Parsons et al. 1984) to establish initial O_2 concentrations, while the remaining bottles were assigned to different light treatments, each with 4 replicates. Light treatments were achieved by varying the number of layers of fiberglass window screening placed over the bottles, plus a dark treatment (i.e. for respiration) in opaque black BOD bottles. The high light treatments were incubated with a single layer of screening (~50% irradiance), designed to saturate photosynthesis but avoid photoinhibition. Low-light treatments were achieved by additional layers of window screening. From 17 Apr to 29 May a single low-light treatment (~25 % irradiance, 2 layers of screening) was included. Subsequently, two low-light treatments were included (13% and 6% irradiance; 3 and 4 layers of screening, respectively) to better resolve the photosynthetic rate at low irradiance. The bottles were placed in a 350 L water bath located outdoors at the laboratory dock. Ambient surface water temperature was maintained by pumping surface seawater though the incubator with a volume replacement time of ~3 minutes. HOBO® pendants logged water temperature in the incubator, confirming that the incubator exhibited similar daily temperature means and ranges as the study site. The average (±SD) residual temperature (incubator – in situ) was 0.29 ± 1.09 °C, n=334 (data not shown).

The experiments began in the early morning 06:30–07:30. Light treatment bottles were terminated near sunset after ~ 12 h by addition of Winkler reagents, whereas dark treatment bottles were terminated the following morning after ~24 h. The longer dark treatment exposures were chosen to improve resolution of the respiration measurements.

Dissolved O_2 concentrations were determined via precision Winkler titration using a MetrOhm Titrando with electrochemical endpoint detection. For each experiment, the thiosulfate titrant calibrated against 5–7 replicates of an iodate standard. To maximize resolution, the entire BOD bottle contents (minus 10.0 ml to allow for titrant) were titrated within the bottle. The variation in individual BOD bottle volumes (range: 296–307 ml, determined gravimetrically) was incorporated in the calculations. The median coefficient of variation in dissolved O_2 concentration among replicate bottles was <1.3% (n = 226).

Net O_2 fluxes were calculated as the difference in dissolved O_2 concentrations between initial and final treatments divided by the incubation period (hours). The net fluxes from the high light treatments yielded maximum net production rates (P_n), whereas negative net fluxes from the dark treatments yielded respiration rates (R_n); for convenience values for R_n were represented as positive values. The maximum gross production rates (P_m) were calculated as:

$$P_m = P_n + R_n \quad (1)$$

Photosynthetic efficiency at low light (α) was calculated as:

$$\alpha = \frac{O_2\ flux\ (low\ light) - O_2\ flux\ (dark)}{Fraction\ of\ \ full\ irradiance\ (low\ light)} \quad (2)$$

Both P_m and α were normalized to photosynthetically active biomass (as Chl-*a*), denoted as $P_m{}^B$, and α^B, for integrating photosynthetic production over the water column of depth H, after Platt et al. (1990):

$$P = \int_{z=0}^{H} B_z * P_m^B \left(1 - e^{-\frac{\alpha^B I_z}{P_m^B}}\right) dz \quad (3)$$

where B_z is the Chl-*a* concentration at depth z, and I_z is irradiance at depth z. At the channel site, B_z was estimated from calibrated CTD fluorescence profiles (Chl-a = 3.87 * Fluorescence - 0.45, $R^2 = 0.77$, N = 36, data not shown), whereas at the shoal site B_z was assumed vertically uniform and equal to the extracted Chl-*a* measurements from surface samples. Irradiance was modeled as:

$$\frac{I_z}{I_0} = e^{-kz} \quad (4)$$

where I_z/I_o is fraction of surface irradiance at depth z. The light attenuation coefficient (k) was calculated as 1.4/Secchi depth, an empirical relationship developed previously for Pensacola Bay from paired CTD PAR profiles and Secchi disk depths ($r^2 = 0.65$, n =487, US EPA unpublished), and similar to those developed elsewhere (e.g., Keefe et al. 1976). To provide a simple index of light availability over the study, water column average irradiance was calculated after Cloern (1999):

$$I_{avg} = I_0/kH(1 - e^{-kH}) \quad (5)$$

Finally, the daily gross production rates were calculated by multiplying P by the number of daylight hours (range: 12.8 to 14.0 h) and daily respiration rates (R_t) were calculated by multiplying the R_n by 24.

Ecosystem Metabolism

We applied the open water method (Odum 1956, Caffrey et al. 2014), which models dissolved O_2 flux at each time step as:

$$\frac{\partial C}{\partial t} = P_e + R_e + D \quad (6)$$

where $\partial C/\partial t C$ is the measured dissolved O_2 flux rate (mmol O_2 m^{-3} h^{-1}), P_e is the photosynthesis rate, R_e is the respiration rate, and D is the volumetric air-sea exchange rate. D was calculated as:

$$D = k_a(C_s - C) \quad (7)$$

where k_a is the volumetric reaeration coefficient (h^{-1}) and C_s is the O_2 saturation concentration as a function of water temperature and salinity (Benson and Krause 1984). For k_a, a modified form of the equation developed by Ro and Hunt (2006) was used, as implemented by Thebault et al. (2008):

$$k_a = \frac{1}{H} \cdot 1.706 \cdot \left(\frac{D_w}{\nu_w}\right)^{\frac{1}{2}} \cdot \left(\frac{\rho_a}{\rho_w}\right)^{\frac{1}{2}} \cdot U_{10}{}^{1.81} \quad (8)$$

where H is water column depth (m), D_w is diffusivity of O_2 in seawater (m^2 s^{-1}), ν_w is the kinematic viscosity of seawater at a given temperature and salinity (m^2 s^{-1}), ρ_a and ρ_w are the densities of air and seawater, respectively (kg m^{-3}), and U_{10} is the wind speed normalized to 10 m above ground level (m s^{-1}).

The diffusion corrected dissolved O_2 fluxes ($\partial C/\partial t C$ - D) were averaged separately over day and night periods to compute apparent primary production (P_a) and nighttime respiration (R_n) rates, respectively. Respiration rates (again, expressed as a positive value herein) were

assumed equal during day and night, thus daily ecosystem respiration (*ER*) was calculated as $R_n \cdot 24 \cdot H$; daily gross ecosystem production (*GPP*) was calculated as (P_a+R_n) * daylight hours * H. Finally, net ecosystem metabolism (*NEM*) was calculated as:

$$NEM = GPP - ER \quad (9)$$

Statistics

Associations among metabolic and environmental parameters were evaluated using Pearson correlation analysis. For continuous *in situ* data, cross correlation analysis (CCA) was used to evaluate the time lags between the synchronous time series at the channel and shoal sites for each of the water quality variables. CCA analyses were run separately for the spring (April – June) and summer (July – September) deployment periods. For CCA, strong correlations with small lag scores indicate that the time series are highly synchronous. Alternatively, lower correlation coefficients imply greater site-to-site variability or independence among variables, while higher lag scores (positive or negative) indicate that one of the time series consistently lagged the other.

A two-way analysis of variance (ANOVA) was performed to test for site (channel/shoal) and seasonal (spring/summer) differences in hourly net production and respiration. Separate models were used to account for the unbalanced sample size among methods (n = 40 incubation method, n = 329 open-water method). Models for the open-water method included an autocorrelation component to account for time-dependence between observations (Pinheiro et al. 2016).

Results

Environmental Conditions

Rainfall during the study (Fig. 2a) was characterized by a wet April (117 mm $month^{-1}$), a dry May (41 mm $month^{-1}$), and a wet summer, with July being exceptional (418 mm $month^{-1}$). River discharge (Fig. 2b) reflected the local precipitation patterns, with relatively high discharge (166 $m^3 s^{-1}$) during April, followed by a sharp decline in May-June (average 62 $m^3 s^{-1}$), near the 25th percentile of long-term averages. The high rainfall was also reflected in the Escambia River hydrograph in July and August (average: 145 $m^3 s^{-1}$), exceeding the 75th percentile of long-term averages. By September, flow decreased to a more normal seasonal pattern.

Overall, surface waters reflected the seasonal warming and increasing influence of freshwater from spring to summer (Table 1). Nitrate concentrations, often below detection, were always < 1 mmol m^{-3}. Ammonium concentrations were also low, ranging from ~0.1 to 1.4 mmol m^{-3} and phosphate concentrations were typically about 0.1 mmol m^{-3}. Silicate varied widely from 6.9 to 67 mmol m^{-3} and was correlated with salinity (Pearson's R = 0.87, P < 0.001, n = 39). Medians and ranges for all variables were similar at the shoal and channel sites (Table 1).

The continuous time series (Fig. 3) also reflected the seasonal warming and freshening of the estuary that occurred at both sites. Temperature increased from ~20° C to ~30° C during May and June, then stayed near 30°C from July to September. Salinity was initially relatively high (~25) during spring then strongly decreased (~15) during summer. The decrease in salinity was accompanied by an increase in FDOM fluorescence (Fig. 3e) and an increase in variability in dissolved O_2 % saturation (Fig. 3c). At the shoal site, dissolved O_2 was persistently supersaturated from April-June, then oscillated between periods of under-saturation and super-saturation, with a sharp peak reaching ~130% on 6 September. At the channel site, dissolved O_2 % saturation was initially lower and less variable than at the shoal site, remaining close to 100% saturation from April-June. In September, the channel site became strongly super-saturated similar to the shoal site. Chl-*a* (Fig. 3d) was low (< 3 mg m^{-3}) from April-June, then noticeably increased in July and peaked in September coinciding with the peak in dissolved O_2 % saturation. FDOM fluorescence strongly co-varied with salinity (Pearson's $R = 0.96$, $P < 0.001$, $n = 330$), reflecting its predominately freshwater origin. The influx of freshwater more than doubled FDOM fluorescence from 14.5 ± 4.2 mg m^{-3} quinine sulfide di-hydrate equivalents (QSDE) from April-June to 34.9 ±7.1 mg m^{-3} QSDE from July-Sept. Wind speeds (Fig. 3g) were typically low over the study, with daily averages ranging from 1.6 to 9.2 m s^{-1}, and daily peaks ranging from 3.4 to 13.0 m s^{-1}. Turbidity (Fig. 3f) was generally low at both sites with a study wide average (± SD) of 1.18 ± 0.54 NTU, however periodic sediment resuspension at the shoal site was evident in the turbidity record (Fig. 3g).

Cross-correlation analysis (Table 2) of the synchronous time series showed that water temperature, salinity, and FDOM were strongly correlated ($r \geq 0.88$ for all) among sites with small lags, reflecting the very similar hydrology. Correlations were lower for the non-conservative variables (dissolved O_2, turbidity, and Chl-*a* fluorescence), suggesting higher site-to-site variability in these measures. For these, the lags varied between −7 to +5 time steps (−3.5 to + 2.5 hours), however the low correlations implied that the lags were not consistent enough over the study period to be meaningful.

At the channel site, the vertical water column structure was visualized with time-space contour plots of the weekly CTD profiles (Fig. 4). Temperature (Fig. 4a) showed clear seasonal warming and appeared vertically uniform. Salinity (Fig. 4b) was relatively high and vertically uniform during the spring, but decreased sharply and became strongly stratified during summer, based on the bottom – surface difference in salinity (Δ salinity > 10). During the period of persistent stratification, the depth of the pycnocline varied from 2 to 4 m (Fig. 4b). Dissolved O_2 (Fig. 4c) reflected the changes in salinity stratification, being vertically uniform from April to June, then showing significant O_2 depletion in the bottom layer in July-August. The lowest dissolved $_{O2}$ concentration of 54.4 mmol m^{-3} (1.7 mg L^{-1} or 26% of saturation), occurred on 4 September. Chl-*a* fluorescence (Fig. 4d) was higher in the bottom layer during spring when the water column was well mixed. With the onset of stratification, surface layer Chl-*a* increased and bottom layer Chl-*a* decreased. On 4 September, a strong mid-depth peak in Chl-*a* was observed, which coincided with the minimum dissolved O_2 concentrations in the bottom layer.

Site and season effects on net production and respiration

A 2-way ANOVA was conducted on light and dark O_2 fluxes (i.e., hourly volumetric net production and respiration, respectively) reasoning that these values represent raw measures, thus do not require the additional scaling assumptions (e.g., integration depth, photosynthetic response to light, air sea O_2 exchange, etc.) needed for estimating areal rates. The results (Table 3) revealed some similarities and differences in response patterns among the bottle experiments and the open water method. For the bottle experiments, there was no significant site effect for either light and dark O_2 fluxes. In contrast, the open water method showed a significant positive site effect, indicating that both light and dark O_2 fluxes were higher at the shoal site. The bottle experiments showed a positive season effect for light O_2 fluxes but not for dark O_2 fluxes, suggesting that net productivity was higher in summer but respiration did not vary seasonally. In contrast, the open water showed a positive season effect for both light and dark O_2 fluxes. The bottle experiments showed no significant site-by-season interaction for light or dark O_2 fluxes, indicating that both sites responded similarly to season. In contrast, the open water method had significant site-by-season effects for both light and dark O_2 fluxes, indicating that the sites responded differently to season.

Water Column Integrated Metabolism

Water column integrated gross production, community respiration, and net metabolism calculated from the bottle experiments are summarized as seasonal averages in Table 4 and shown as time series in Fig. 5. Both water column production and respiration were consistently about 3 fold higher at the channel site than the shoal site owing primarily to the deeper water column depth (Fig. 5). Over the study, water column gross production averaged (± SE) 42.1 ± 6.5 mmol O_2 m^{-2} d^{-1} at the shoal site and 125.7 ± 20.2 mmol O_2 m^{-2} d^{-1} at the channel site, and correlated positively with Chl-*a* (Table 5). Similarly, water column respiration rates averaged of 23.6 ± 2.6 mmol O_2 m^{-2} d^{-1} at the shoal site and 81.7 ± 9.1 mmol O_2 m^{-2} d^{-1} at the channel site. Seasonal averages (Table 4) show that water column production and respiration both increased from spring to summer, a pattern more pronounced at the channel site, where gross production peaked at over 250 mmol O_2 m^{-2} d^{-1}. Net water column metabolism (Fig. 5) ranged widely from −98.9 to 267.4 mmol O_2 m^{-2} d^{-1} with both extremes occurring at the channel site. During spring, net metabolism was near balanced at both sites, then became consistently autotrophic during the summer, especially at the channel site. Averaged across both sites, water column P:R ratios increased from 1.28 to 4.86 from spring to summer.

Ecosystem Integrated Metabolism

Integrated ecosystem gross production, respiration and net metabolism are shown as time series in Fig. 6, and seasonal averages shown in Table 4. While air-sea exchange was calculated as described in the methods, it should be noted that it was typically small component of integrated ecosystem metabolism rates (range: −3.5 to +1.2 mmol O_2 m^{-2} d^{-1}), representing an average (± SE) of 8.8 ± 2.1 % of net O_2 fluxes at the shoal site and 0.2 ± 0.41 % at the channel site (data not shown). Ecosystem production and respiration were tightly coupled at both shoal and channel sites (Pearson's R: 0.92 and 0.93, respectively, n = 154 each), and P:R ratios ranged narrowly from 0.84 to 1.16. Averaged across both sites,

ecosystem production averaged 196.8 mmol O_2 m^{-2} d^{-1} (range: 29.6 – 517.0 mmol O_2 m^{-2} d^{-1}) and ecosystem respiration averaged 198.3 mmol O_2 m^{-2} d^{-1} (range: 44.4 – 563.3 mmol O_2 m^{-2} d^{-1}). However, each site had a distinct seasonal pattern. At the shoal site, ecosystem gross production and respiration both decreased slightly (Table 4), whereas at the channel site, ecosystem gross production and respiration both increased sharply from spring to summer (e.g., ecosystem production increased from 110.2 to 283.4 mmol O_2 m^{-2} d^{-1}). Strong peaks in ecosystem production and respiration were observed at the channel site in late August and early September, after which they declined to levels similar to the shoal site. Thus, ecosystem production and respiration exhibited an apparent strong seasonal increase at the channel site, but not at shoal site. The time series also showed noticeable oscillations in metabolic rates with approximately semi-monthly frequency, a pattern that was more pronounced at the shoal site. However, the oscillations appeared out of phase, such that peaks and valleys occurred at different times at the channel and shoal sites.

Net ecosystem metabolism (Fig. 6, Table 4) exhibited site specific differences. At the shoal site, net ecosystem metabolism was slightly positive during spring, averaging 11.5 mmol O_2 m^{-2} d^{-1}, then decreased to an average of −0.5 mmol O_2 m^{-2} d^{-1} during summer. At the channel site, net ecosystem metabolism remained near balanced throughout the study, ranging from −3.3 to 0.3 mmol O_2 m^{-2} d^{-1}. During late August and early September, net metabolism varied widely at both sites, becoming strongly autotrophic then strongly heterotrophic for brief periods. This period of high variability coincided with the strong peak in ecosystem production and respiration at the channel site.

Residual Metabolism

The coordinated measurements of water column and ecosystem metabolism allowed us calculate residual production and respiration rates, defined as the difference between ecosystem and water column integrated rates. The time series (Fig. 7) and seasonal averages (Table 4) show marked differences among the sites. At the shoal site, residual metabolism (both production and respiration) was initially high in spring then declined during summer. In contrast, residual metabolism at the channel site was low in spring and during summer. Residual gross production at the shoal site was positively correlated to salinity and average water column irradiance (Table 5). To illustrate the contrast in responses to environmental variability among sites, we show relationships (Fig. 8) between residual gross production and respiration and the water column average irradiance (I_{avg}, Figs. 8a and 8b) and water column stratification, measured as the difference in salinity between surface and bottom waters (Δ *salinity*, Figs. 8c and 8d). At the shoal site (Figs. 8a and 8b), residual production and respiration were positively related to I_{avg}, but not Δ *salinity*. Conversely, at the channel site, residual production and respiration were positively related to Δ *salinity* (though only marginally so, $P < 0.10$ and $P < 0.12$, respectively), but not water column irradiance. Thus, it appeared that the environmental drivers of residual metabolism were site-specific and related to light and stratification conditions.

Discussion

Methodological considerations

Despite many decades of research aimed at quantifying coastal ecosystem primary productivity, there is no consensus on best practices, making global assessments challenging (Cloern et al. 2014). The advent of increasingly reliable electronic instrumentation holds promise for making 'incubation-free' (i.e., open water) productivity measurements, which are logistically much simpler than controlled experimental incubations. However, both incubation and incubation-free methods rely on simplifying assumptions, which if violated, may lead to inaccurate or misleading interpretations (Kemp and Testa 2012). Here, we consider some key assumptions for each approach used here.

Both the incubation and incubation-free methods used here were O_2 based, facilitating comparisons to each other. However, to calculate daily integrated gross productivity rates, one must estimate O_2 consumption (i.e. respiration) during daylight hours. We assumed that respiration rates during the night (open water method) or in dark bottles (incubation method) were reasonable estimates of daytime respiration rates. While it is well known that phytoplankton respiration rates are sensitive to the prevailing light environment (e.g., Grande et al. 1989), typically being higher in the light than in the dark, we assumed the difference to be negligible. If phytoplankton respiration rates were indeed higher during daylight hours, then our assumption of uniform respiration rates would result in underestimating daily integrated both gross production and respiration rates, but should not affect net metabolism.

Both methods used here also assumed that O_2 production was solely attributable to photoautotrophs. However, in certain environments, chemoautotrophic nitrifying bacteria, which consume O_2 and fix CO_2, may complicate estimates. If significant, then ignoring nitrification would result in overestimating respiration rates and underestimating net carbon production rates. Such an artifact would be expected to be greatest in light-limited, high NH_4^+ environments (e.g., Gazeau et al. 2005). Based on the empirical relationship reported in Berounsky and Nixon (1993), we estimated that water column nitrification may account for 3–5% of O_2 consumption in Pensacola Bay, similar to other low nutrient estuaries (Damashek et al. 2016, Table 2). For sediments, potential nitrification rates measured in surficial sediments from Pensacola Bay were generally low, typically < 0.5 μmol N g^{-1} d^{-1} (Caffrey et al. 2007, Smith and Caffrey 2009). If assumed representative of the top 0.5 cm of sediment, benthic nitrification may account for 9% of benthic O_2 consumption in the seagrass meadow and 30% in bare sediments. Combining water-column and potential sediment rates, we estimated that nitrification rates may account for 2% and 6% of the O_2 flux at the seagrass and bare sediment sites, respectively. Given this estimate and that Pensacola Bay waters generally have high light transparency and very low NH_4^+ concentrations, nitrification was likely a minor source of error in metabolism estimates in this study.

All bottle incubation methods assume that enclosing water samples will not fundamentally alter plankton activities, thus derived production and respiration rate estimates are deemed representative of *in situ* conditions. However, isolating plankton from exogenous sources of nutrients and organic matter may alter primary production and respiration, respectively.

During the course of an incubation, nutrient limitation may decrease autotrophic O_2 production, while organic matter depletion may decrease heterotrophic O_2 consumption. Based on the observed low nutrient concentrations and the results from nutrient addition experiments conducted in parallel to this study (data not shown), it is likely that phytoplankton did become nutrient limited, consistent with an earlier study in lower Pensacola Bay (Juhl and Murrell 2008). However, Juhl and Murrell (2008) also found that development of nutrient limitation during 48 h incubations was not severe enough to reduce photosynthetic efficiency, implying that O_2 fluxes may not be strongly affected by nutrient depletion in our ~12 hour incubations. As for organic matter limitation, several time course experiments conducted in Pensacola Bay (Murrell, unpublished) indicated that O_2 consumption rates were constant for 48–72 hours following collection, a finding consistent with other researchers (e.g., Robinson et al. 2005). So, while plankton may become nutrient and/or organic matter limited during the course of an incubation, the effect on O_2 fluxes appears to be small for the first 24–48 hours.

Incubations experiments may also be affected by uneven capture of rare and large plankton in the BOD bottles. Clearly, large zooplankton (nominal abundances of 1–5 L^{-1}) will not be evenly distributed among 300 ml sample volumes. Such an artifact, if important, would be expected to cause high variability in O_2 fluxes among replicate bottles, but not necessarily create a directional bias. During our experiments, variability among replicates was small (median coefficient of variation <1.3%, n = 226) and similar in both light and dark treatments, suggesting that uneven capture of rare zooplankton was likely a minor source of error.

A final limitation of incubation methods considered here is the common practice, especially in shallow systems, of collecting and incubating water samples taken from a single depth, and assuming that it represents plankton processes in the entire water column. If phytoplankton biomass or their photosynthetic characteristics are vertically heterogeneous, then errors in integrated productivity estimates may result. For productivity, we partly compensated for this variability by incorporating the vertical distribution of Chl-a (from calibrated CTD fluorescence profiles) and irradiance (from modeled light profiles) into the integrated productivity estimates. For respiration, surface-only measurements may not accurately reflect water column conditions, and may overestimate true respiration rates because surface waters tend to have higher respiration rates than bottom waters, especially when the water column is stratified (e.g., Murrell et al. 2013). Clearly, a more complete picture of the vertical distribution of phytoplankton and heterotrophic plankton would improve estimates of water column metabolism.

Implementing the open water O_2 method also requires simplifying assumptions, which have been discussed extensively in the literature (Kosinski 1984, Hanson et al. 2008, Staehr et al. 2010, Needoba et al. 2012) and a full discussion is beyond the scope of this paper. Instead, we will focus on a key assumption that most likely affected results of this study, namely that the water mass was homogeneous both horizontally and vertically. In many systems, especially in conjunction with long-term monitoring programs (e.g. National Estuarine Research Reserves System Wide Monitoring Program), *in situ* sensors are commonly deployed at a single water depth and assumed representative of the water column for

calculating ecosystem metabolism rates. In very shallow systems, this approach is often justified (e.g., Caffrey 2004), however it is important to recognize that even in shallow systems, particularly microtidal estuaries, the water column may become stratified. Stratification can lead to systematic errors in open water integrated estimates. Process rates below above and below a pycnocline may differ and, depending on the sensor placement, the resulting estimates may not capture benthic processes. Several studies have attempted to overcome this limitation by deploying sensors at multiple water depths and applying more complex models to calculate metabolism (Staehr et al. 2012, Champenois and Borges 2012, Obradour et al. 2014, Tonetta et al. 2016). Thus, it is important to recognize that if stratification conditions are unknown or insufficiently characterized, then errors in integrated metabolism derived from O_2 time series may result.

Residual Metabolism at the Shoal Site

The residual metabolism estimates calculated in this study provide a means of partially evaluating key assumptions of the methods described above. At the shoal site, residual production and respiration rates were relatively large and consistent, consistent with the expectation that the water column was a relatively small component of total ecosystem metabolism. In this sense, these results were similar to Ziegler and Benner (1998) in the Laguna Madre (Texas, USA) and to Champenois and Borges (2012) in the Bay of Revellata (Corsica, France). Additionally, the magnitudes of residual rates, averaging 138 mmol O_2 m $^{-2}$ d^{-1} and 152 mmol O_2 m^{-2} d^{-1} for gross production and respiration, respectively, were similar to benthic rates measured in chambers deployed in seagrass meadows (Murray and Wetzel 1987, Ziegler and Benner 1998, Yarbro and Carlson 2008, Nagel et al. 2009, Hester et al. 2016). Residual gross production rates at the shoal site (Fig 8a) were low in spring, peaked in summer, then declined in late summer and fall. This seasonal progression is similar to seagrass productivity estimates derived from chamber incubations in other sub-tropical seagrass ecosystems (Stutes et al. 2007, Yarbro and Carlson 2008, Hester et al. 2016). Residual gross production was also significantly correlated with I_{avg} ($r = 0.62$, $P<0.004$), similar to other seagrass ecosystems (e.g., Herzka and Dunton 1996, Hester et al. 2016). Taken together, the magnitude and seasonality of residual gross production and respiration compare favorably to the direct benthic measurements from similar seagrass environments reported in the literature.

Residual Metabolism at the Channel Site

Residual metabolism at the channel site revealed a more complex picture (see Fig. 7) than the shoal site. During spring, residual gross production and respiration rates were low, averaging 15.7 and 36.7 mmol O_2 m^{-2} d^{-1}, respectively. This is consistent with modest benthic metabolism expected for bare sediments with relatively low light availability (in our case, 3–15 % of surface irradiance) and low benthic biomass compared to a seagrass meadow. Further, these rates of residual metabolism were similar in magnitude to benthic gross production and respiration rates measured previously in Pensacola Bay (Murrell et al. 2009). However, with the onset of water column stratification, residual metabolism at the channel site increased sharply, averaging 86.7 ± 43.2 mmol m^{-2} d^{-1} and 201.7 ± 45.4 mmol m^{-2} d^{-1} for gross production and respiration rates, respectively, and well outside of norms for bare sediment benthic environments. During this summer period, sediments were more

severely light limited (0.2 to 6 % of surface irradiance) than during spring, further minimizing the likelihood of significant benthic productivity. Similarly, the calculated residual respiration rates (> 200 mmol m^{-2} d^{-1}) far exceeded comparable direct measurements from estuaries (Middelburg et al. 2005, Murrell et al. 2009). Thus, it appears likely that the strong diel O_2 fluctuations observed during this period only reflected processes in the surface layer but were attributed to the entire water column in the open water model, thus likely overestimating ecosystem production and respiration rates. This interpretation is supported by the positive relationship between the strength of stratification and the magnitude of residual metabolism (Fig. 8b). The problem of stratification has been recognized in several estuarine (Swaney et al. 1999) and lake studies (Coloso et al. 2008, Staehr et al. 2012, Obrador et al. 2014, Tonetta et al. 2016) and require additional O_2 sensors deployed throughout the water column to improve estimates. Thus the high summer residual metabolism observed at the channel site appeared to reflect a limitation in our sampling design, and estimates of integrated production and respiration at this site during stratification should be viewed with caution.

To partially account for this limitation and to better constrain ecosystem gross production and respiration rates during the stratified period, we summed estimates of three component measures separately, namely the surface water column, the lower water column, and the benthos (see Table 6). This analysis was restricted to the seven dates at the channel site during the stratified period (delta salinity > 10) and a clear pycnocline could be identified from the CTD profiles. We used data from this study combined with information from a prior Pensacola Bay study (Murrell et al. 2009) as follows. Surface layer gross primary production and respiration rates were calculated via the open water method by restricting the integration depth to the surface mixed layer as defined by the pycnocline (shown in Fig. 4b). Thus, instead of assuming the full water column depth (6 m), the pycnocline depth (~2–3 m) served as the bottom boundary for open water calculations. Below the pycnocline, gross production rates were calculated from the bottle-based rates integrated for the lower water column, accounting for vertical light and Chl-*a* variability. For respiration we assumed uniform respiration rates throughout the water column, thus multiplied the volumetric rates by the depth of the upper and lower portions of the water column. Benthic gross production rates were estimated from the light-dependent relationship described in Murrell et al. (2009): Benthic Gross Production = 0.801 * % Surface Irradiance. Similarly, benthic respiration was assumed to be 11.3 mmol O_2 m^{-2} d^{-1}, the mean value reported in Murrell et al. (2009). The results of this exercise (see Table 6) indicated that the sum of the component-based production and respiration rates (average 221 and 204.6 mmol O_2 m^{-2} d^{-1}, respectively) were consistently lower than the open water rates (average 303.5 and 312.6 mmol O_2 m^{-2} d^{-1}). This comparison supports the argument that open water method overestimated true production and respiration rates (by 37% and 53%, respectively) when the water column was stratified. This result is perhaps not surprising in retrospect, given that water column stratification represents a clear violation of the open water theory.

Drivers of water column and ecosystem metabolism

In this study, the dominant factors driving metabolic rates were the seasonal changes in freshwater flow and temperature resulting in a phytoplankton bloom which affected each site

slightly differently. This is a common response in estuaries (Rudek et al. 1991, O'Donohue and Dennison 1997, Murrell et al. 2007, Ho et al. 2010) and in our case, led to a doubling of water column integrated primary production at the channel site (Table 3). The importance of phytoplankton at the channel site is also reflected in the significant correlations between ecosystem gross production and Chl-*a* and salinity (Table 5), a pattern observed in other estuaries (Kemp et al. 1992, Kemp and Testa 2011). Increased phytoplankton biomass and production can also stimulate community respiration (Hopkinson and Smith 2005), which was apparent in the correlation between ecosystem respiration and Chl-*a* at the channel site. While water column production increased similarly at the shoal site following the summer freshwater flow event, there was an overall decline in ecosystem gross production, suggesting a decrease in benthic productivity. A similar decline ecosystem productivity was observed by Twilley et al. (1985) in SAV beds following nutrient additions, which resulted in increased phytoplankton and epiphyte productivity, but was insufficient to compensate for shading effects on the submersed aquatic vegetation.

In general, the metabolic rates measured in this study fell within the ranges reported from other estuaries (Caffrey 2004, Hopkinson and Smith 2005). Rates of primary production compared well with previous studies of Pensacola Bay (Murrell et al. 2007, Murrell et al. 2009) and other Gulf of Mexico estuarine environments (Pennock et al. 1999, Mortazavi et al. 2000, Lehrter et al. 2009). Similarly, respiration rates from this study were similar to those reported for Pensacola Bay (Murrell et al. 2009) and for estuaries worldwide (Hopkinson and Smith 2005). Thus, Pensacola Bay represents a good model system to examine how human impacts from local and regional landscape level changes as well as global climate change impact estuarine function.

Concluding Remarks

This study illustrated how the two independent approaches to measure primary production and respiration rates helped compartmentalize these processes, and provided a means to evaluate the water column- and ecosystem-level responses to seasonal changes in temperature, hydrology, and light availability. In this study, the open water method appeared to provide reasonable estimates of ecosystem production and respiration in a seagrass meadow, capturing both water column and benthic processes. Similarly, in deeper locations when the water the column was well mixed, the open water and bottle incubation methods largely agreed suggesting the open water method provided reasonable estimates. However, with the onset of water column stratification the two approaches diverged sharply implying potential errors, mostly attributable to violation of a key assumption of the open water method. Increasingly, *in-situ* datasondes are an attractive option for routine monitoring and for assessing ecosystem metabolism, being generally less labor intensive and requiring less expertise than water column or benthic incubation methods. However, caveats (site location, sample collection location, assumptions of method) need to be carefully considered, and ancillary data (CTD profiles, experimental manipulations) are key to evaluating estimates derived from O_2 time series data. Thus, careful application of these methods has the potential to help address the grand challenge proposed by Cloern (2014) in developing globally consistent approaches for characterizing coastal ecosystem productivity.

Acknowledgments

This project was made possible by an excellent support team: Jessica Aukamp, David Beddick, George Craven, Ally Duffy, and Diane Yates. Stephanie Friedman, Susan Yee, Kim Cressman and Yongshan Yan provided comments that improved the manuscript. We also thank four anonymous reviewers and the associate editor for their detailed and insightful comments and suggestions. This study was funded by the US Environmental Protection Agency (US EPA) and has been reviewed and approved for publication. The views expressed here are solely those of the authors, thus do not necessarily reflect the views or policies of the US EPA. Mention of trade names or commercial products does not constitute endorsement by the authors or the US EPA.

Literature Cited

APHA. Standard methods for the examination of water and wastewater APHA (American Public Health Association). Washington, DC: 2005.

Beck MW, Hagy JDI, Murrell MC. Improving estimates of ecosystem metabolism by reducing effects of tidal advection on dissolved oxygen time series. Limnology and Oceanography: Methods. 2015

Benson BB, Krause D Jr. The concentration and isotopic fractionation of oxygen dissolved in freshwater and seawater in equilibrium with the atmosphere. Limnology and Oceanography. 1984; 29:620–632.

Berounsky VM, Nixon SW. Rates of nitrification along an estuarine gradient in Narragansett Bay. Estuaries. 1993; 16:718–730.

Caffrey JM. Factors controlling net ecosystem metabolism in U. S. estuaries. Estuaries. 2004; 27:90–101.

Caffrey JM, Bano N, Kalanetra K, Hollibaugh JT. Ammonia oxidation and ammonia-oxidizing bacteria and archaea from estuaries with differing histories of hypoxia. International Society for Microbial Ecology. 2007; 1:660–662.

Caffrey JM, Murrell MC, Amacker KS, Harper JW, Phipps S, Woodrey MS. Seasonal and inter-annual patterns in primary production, respiration, and net ecosystem metabolism in three estuaries in the northeast Gulf of Mexico. Estuaries and Coasts. 2014; 37:222–241.

Cai W-J. Estuarine and coastal ocean carbon paradox: CO2 sinks or sites of terrestrial carbon incineration? Annual Review of Marine Science. 2011; 3:123–145.

Champenois W, Borges AV. Seasonal and interannual variations of community metabolism rates of a Posidonia oceanica seagrass meadow. Limnology & Oceanography. 2012; 57:347–361.

Cloern JE. The relative importance of light and nutrient limitation of phytoplankton growth: a simple index of coastal ecosystem sensitivity to nutrient enrichment. Aquatic Ecology. 1999; 33:3–16.

Cloern JE, Foster SQ, Kleckner AE. Phytoplankton primary production in the world's estuarine-coastal ecosystems. Biogeosciences. 2014; 11:2477–2501.

Coloso JJ, Cole JJ, Hanson PC, Pace ML. Depth-integrated, continuous estimates of metabolism in a clear-water lake. Canadian Journal of Fisheries and Aquatic Sciences. 2008; 65:712–722.

Costanza R, d'Arge R, de Groot R, Farber S, Grasso M, Hannon B, Naeem S, Limburg K, Paruelo J, O'Neill RV, Raskin R, Sutton P, van den Belt M. The value of the world's ecosystem services and natural capital. Nature. 1997; 387:253–260.

Damashek J, Casciotti KL, Francis CA. Variable nitrification rates across environmental gradients in turbid, nutrient-rich estuary waters of San Francisco Bay. Estuaries and Coasts. 2016; 39:1050–1071.

Gazeau F, Gattuso J-P, Middelburg JJ, Brion L-S, Frankignoulle M, Borges AV. Planktonic and whole system metabolism in a nutrient-rich Estuary (the Scheldt Estuary). Estuaries. 2005; 28:868–883.

Grande KD, Marra J, Langdon C, Heinemann K, Bender ML. Rates of respiration in the light measured in marine phytoplankton using an $^{18}0$ isotope-labelling technique. Journal of Experimental Marine Biology and Ecology. 1989; 129:95–120.

Hagy JD III, Murrell MC. Susceptibility of a Gulf of Mexico estuary to hypoxia: An analysis using box models. Estuarine, Coastal and Shelf Science. 2007; 74:239–253.

Handley, L., Altsman, D., DeMay, R. U.S. Geological Survey Investigations Report 2006–5287 and U.S. Environmental Protection Agency 855-R-04-003. Washington, DC: 2007. Seagrass status and trends in the northern Gulf of Mexico: 1940–2002.

Hanson PC, Carpenter SR, Kimura N, Wu C, Cornelius SP, Kratz TK. Evaluation of metabolism models for free-water dissolved oxygen methods in lakes. Limnology and Oceanography Methods. 2008; 6:454–465.

Herzka S, Dunton KH. Seasonal photosynthetic patterns of the seagrass Thalassia testudinum in the western Gulf of Mexico. Marine Ecology Progress Series. 1997; 152:103–117.

Hester CM, Smith HM, Head ME, Langsten H, Linder S, Manor E, Norman J, Sartory L, Caffrey JM. Comparing productivity and biogeochemistry of native and transplanted Thlassia testudinum and Halodule beaudettei in Big Lagoon, Florida, USA. Gulf of Mexico Science. 2016; 33:14–25.

Ho AY, Xu J, Yin K, Jiang Y, Yuan X, He L, Harrison PJ. Phytoplankton biomass and production in subtropical Hong Kong waters: influence of the Pearl River outflow. Estuaries and Coasts. 2010; 33:170–181.

Holmes RM, Amino A, Kerouel R, Hooker BA, Peterson BJ. A simple and precise method for measuring ammonium in marine and freshwater ecosystems. Canadian Journal of Fisheries and Aquatic Sciences. 1999; 56:1801–1808.

Hopkinson, CS., Jr, Smith, EM. Estuarine respiration: an overview of benthic, pelagic, and whole system respiration. In: del Giorgio, PA., Williams, PJlB, editors. Respiration in aquatic systems. Oxford University Press; Oxford: 2005. p. 122-146.

Juhl AR, Murrell MC. Nutrient limitation of phytoplankton growth and physiology in a subtropical estuary. Bulletin of Marine Science. 2008; 82:59–82.

Keefe CW, Flemer DA, Hamilton DH. Seston distribution in the Patuxent River Estuary. Chesapeake Science. 1976; 17:56–59.

Kemp WM, Testa JM. Metabolic balance between ecosystem production and consumption. Treatise on Estuarine and Coastal Science. 2011:7.

Kemp WM, Sampou PA, Garber J, Tuttle J, Boynton WR. Seasonal depletion of oxygen from bottom waters of Chesapeake Bay: roles of benthic and planktonic respiration and physical exchange processes. Marine Ecology Progress Series. 1992; 85:137–152.

Kosinski RJ. A comparison of the accuracy and precision of several open-water oxygen productivity techniques. Hydrobiologia. 1984; 119:139–148.

Lehrter JC, Murrell MC, Kurtz JC. Interactions between Mississippi River inputs, light, and phytoplankton biomass and phytoplankton production on the Louisiana continental shelf. Continental Shelf Research. 2009; 29:1861–1872.

Middelburg, JJ., Duarte, CM., Gattuso, J-P. Respiration in coastal benthic communities. In: del Giorgio, PA., Williams, PJlB, editors. Respiration in aquatic systems. Oxford University Press; Oxford: 2005. p. 206-224.

Mortazavi B, Iverson RL, Landing WM, Lewis FG, Huang W. Control of phytoplankton production and biomass in a river-dominated estuary: Apalachicola Bay, Florida, USA. Marine Ecology Progress Series. 2000; 198:19–31.

Murray L, Wetzel RL. Oxygen production and consumption associated with the major autotrophic components in two temperate seagrass communities. Marine Ecology Progress Series. 1987; 38:231–239.

Murrell MC, Hagy JD, Lores EM, Greene RM. Phytoplankton production and nutrient distributions in a sub-tropical estuary: importance of freshwater flow. Estuaries and Coasts. 2007; 30:390–402.

Murrell MC, Campbell JG, Hagy JD III, Caffrey JM. Effects of irradiance on benthic and water column processes in a Gulf of Mexico estuary: Pensacola Bay, Florida, USA. Estuarine, Coastal and Shelf Science. 2009; 81:501–512.

Murrell MC, Stanley RS, Lehrter JC, Hagy JD. Plankton community respiration, net ecosystem metabolism, and oxygen dynamics on the Louisiana continental shelf: implications for hypoxia. Continental Shelf Research. 2013; 52:27–38.

Nagel JL, Kemp WM, Cornwell JC, Owens MS, Hinkle D, Madden CJ. Seasonal and regional variations in net ecosystem production in Thalassia testudinum communities throughout Florida Bay. Contributions in Marine Science. 2009; 38:91–108.

Needoba, JA., Peterson, TD., Johnson, KM. Method for the quantification of aquatic primary production and net ecosystem metabolism using in situ dissolved oxygen sensors. In: Tiquia-

Arashiro, SM., editor. Molecular biological technologies for ocean sensing. Springer Protocols Handbooks; New York: 2012.

Nidzieko NJ, Needoba JA, Monismith SG, Johnson KM. Fortnightly tidal modulations affect net community production in a mesotidal estuary. Estuaries and Coasts. 2014

O'Donohue MJ, Dennison WC. Phytoplankton productivity response to nutrient concentrations, light availability and temperature along an Australian estuarine gradient. Estuaries. 1997; 20:521–533.

Obrador B, Staehr PA, Christensen JPA. Vertical patterns of metabolism in three contrasting stratified lakes. Limnology & Oceanography. 2014; 59:1228–1240.

Odum HT. Primary production in flowing waters. Limnology and Oceanography. 1956; 1:102–117.

Parsons, TR., Maita, Y., Lalli, CM. A manual of chemical and biological methods for seawater analysis. Pergamon Press; New York: 1984.

Pennock, JR., Boyer, JN., Herrera-Silveira, JA., Iverson, RL., Whitledge, TE., Mortazavi, B., Comin, FA. Nutrient behavior and phytoplankton production in Gulf of Mexico estuaries. In: Bianchi, TS.Pennock, JR., Twilley, RR., editors. Biogeochemistry of Gulf of Mexico Estuaries. John Wiley and Sons, Inc; New York: 1999. p. 109-162.

Pinheiro, J., Bates, D., DebRoy, S., Sarkar, D. R Core Team. Linear and Nonlinear Mixed Effects Models. R package version 3.1-128. 2016. http://CRAN.R-project.org/package=nlme

Platt T, Sathyendranath S, Ravindran P. Primary production by phytoplankton: analytic solutions for the daily rates per unit area of water surface. Proceedings of the Royal Society London B: Biological Sciences. 1990; 241:101–111.

Ro KS, Hunt PG. A new unified equation for wind-driven surficial oxygen transfer into stationary water bodies. Transactions of the American Society of Agricultural and Biological Engineers. 2006; 49:1615–1622.

Robinson, C., Williams, PJlB. Respiration and its measurements in surface marine waters. In: del Giorgio, PA., Williams, PJlB, editors. Respiration in aquatic systems. Oxford University Press; Oxford: 2005. p. 147-180.

Rudek J, Paerl HW, Mallin MA, Bates PW. Seasonal and hydrological control of phytoplankton nutrient limitation in the lower Neuse River Estuary, North Carolina. Marine Ecology Progress Series. 1991; 75:133–142.

Smith SV, Hollibaugh JT. Coastal metabolism and the oceanic organic carbon balance. Reviews of Geophysics. 1993; 31:75–89.

Smith KA, Caffrey JM. The effects of human activities and extreme meteorological events on sediment nitrogen dynamics in an urban estuary, Escambia Bay, Florida, USA. Hydrobiologia. 2009; 627:67–85.

Sokal, RR., Rohlf, FJ. Biometry. 3. W H Freeman and Co; 1995.

Staehr PA, Sand-Jensen K. Temporal dynamics and regulation of lake metabolism. Limnology & Oceanography. 2007; 52:108–120.

Staehr PA, Sand-Jensen K, Raun AL, Nilsson B, Kidmose J. Drivers of metabolism and net heterotrophy in contrasting lakes. Limnology & Oceanography. 2010; 55:817–830.

Staehr PA, Testa JM, Kemp WM, Cole JJ, Sand-Jensen K, Smith SV. The metabolism of aquatic ecosystems: history, applications and future challenges. Aquatic Sciences. 2012; 74:15–29.

Stutes J, Cebrian J, Stutes AL, Hunter A, Corcoran AA. Benthic metabolism across a gradient of anthropogenic impact in three shallow coastal lagoons in NW Florida. Marine Ecology Progress Series. 2007; 348:55–70.

Swaney DP, Howarth RW, Butler TJ. A novel approach for estimating ecosystem production and respiration in estuaries: Application to the oligohaline and mesohaline Hudson River. Limnology & Oceanography. 1999; 44:1509–1521.

Thèbault J, Schraga TS, Cloern JE, Dunlavey EG. Primary production and carrying capacity of former salt ponds after reconnection to San Francisco Bay. Wetlands. 2008; 28:841–851.

Thorpe, P., Bartel, R., Ryan, P., Albertson, K., Pratt, T., Cairns, D., Sultana, F., Macmillan, T., Culbertson, M., Montford, H. The Pensacola Bay system surface water improvement and management plan. Northwest Florida Water Management District; Crestview, FL: 1997. http://www.nwfwmd.state.fl.us/water-resources/swim/pensacola-bay/

Tonetta D, Staehr PA, Schmitt R, Mello Petrucio M. Physical conditions driving the spatial and temporal variability in aquatic metabolism of a subtropical coastal lake. Limnologica. 2016; 28:30–40.

Twilley RR, Kemp WM, Staver KW, Stevenson JC, Boynton WR. Nutrient enrichment of estuarine submersed vascular plant communities. 1. Algal growth and effects on production of plants and associated communities. Marine Ecology Progress Series. 1985; 23:179–191.

US EPA (US Environmental Protection Agency). The ecological condition of the Pensacola Bay system, northwest Florida (1994–2001). US Environmental Protection Agency; 2005.

Welschmeyer NA. Fluorometric analysis of chlorophyll-a in the presence of chlorophyll-b and phaeopigments. Limnology and Oceanography. 1994; 39:1985–1992.

Williams, PJlB, Quay, PD., Westberry, TK., Behrenfeld, MJ. The oligotrophic ocean is autotrophic. Annual Review of Marine Science. 2013; 5:535–549.

Yarbo LA, Carlson PR. Community oxygen and nutrient fluxes in seagrass beds of Florida Bay, USA. Estuaries and Coasts. 2008; 31:877–897.

Ziegler S, Benner R. Ecosystem metabolism in a subtropical, seagrass-dominated lagoon. Marine Ecology Progress Series. 1998; 173:1–12.

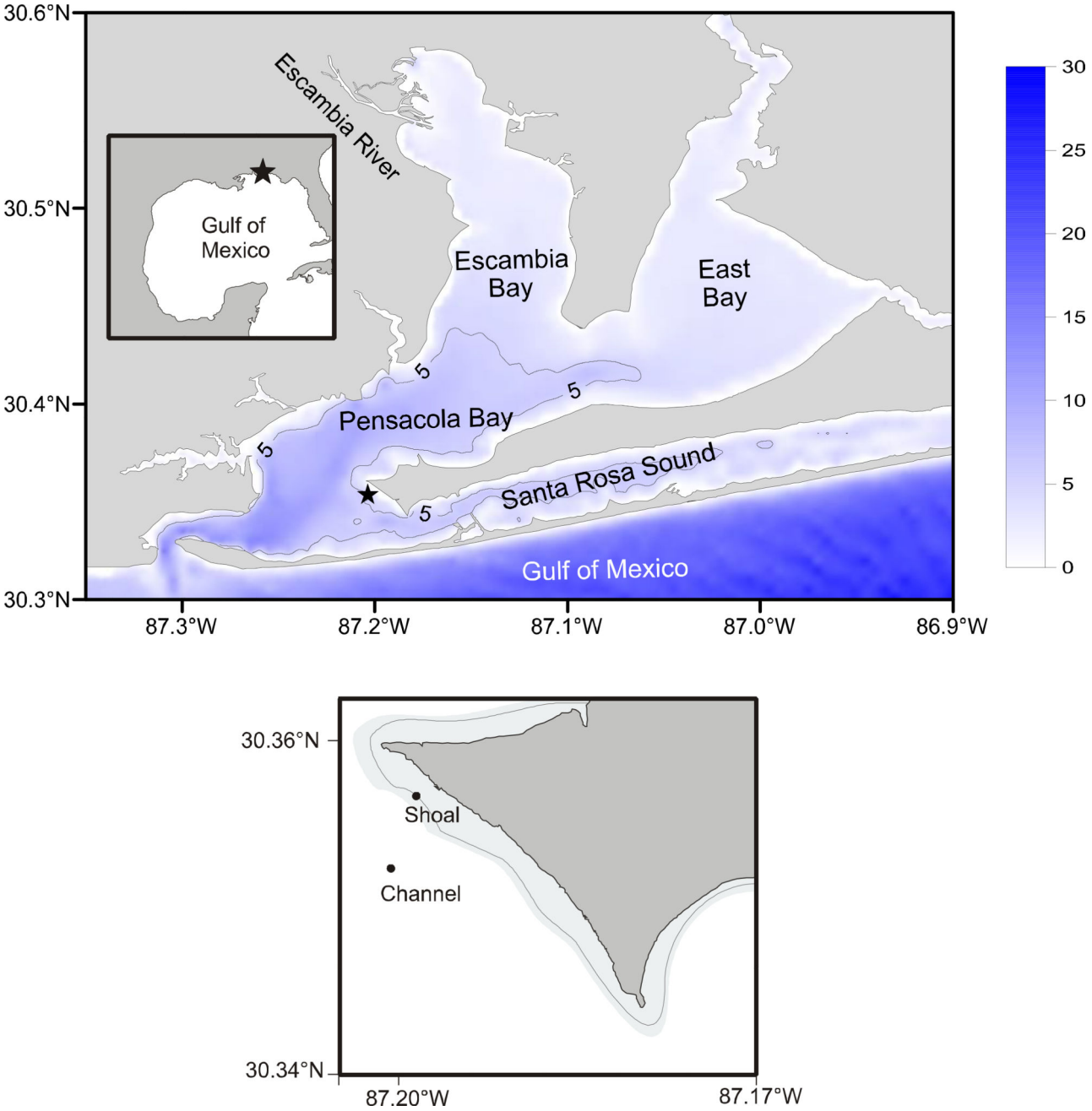

Figure 1.

Map of Pensacola Bay estuary located in the northern Gulf of Mexico (*inset*). Shading and color bar depicts water depth (m), including the 5 m contour (*contour line*). The lower map shows detail of the sampling sites; the approximate distribution of seagrasses is shown with shading and a line border.

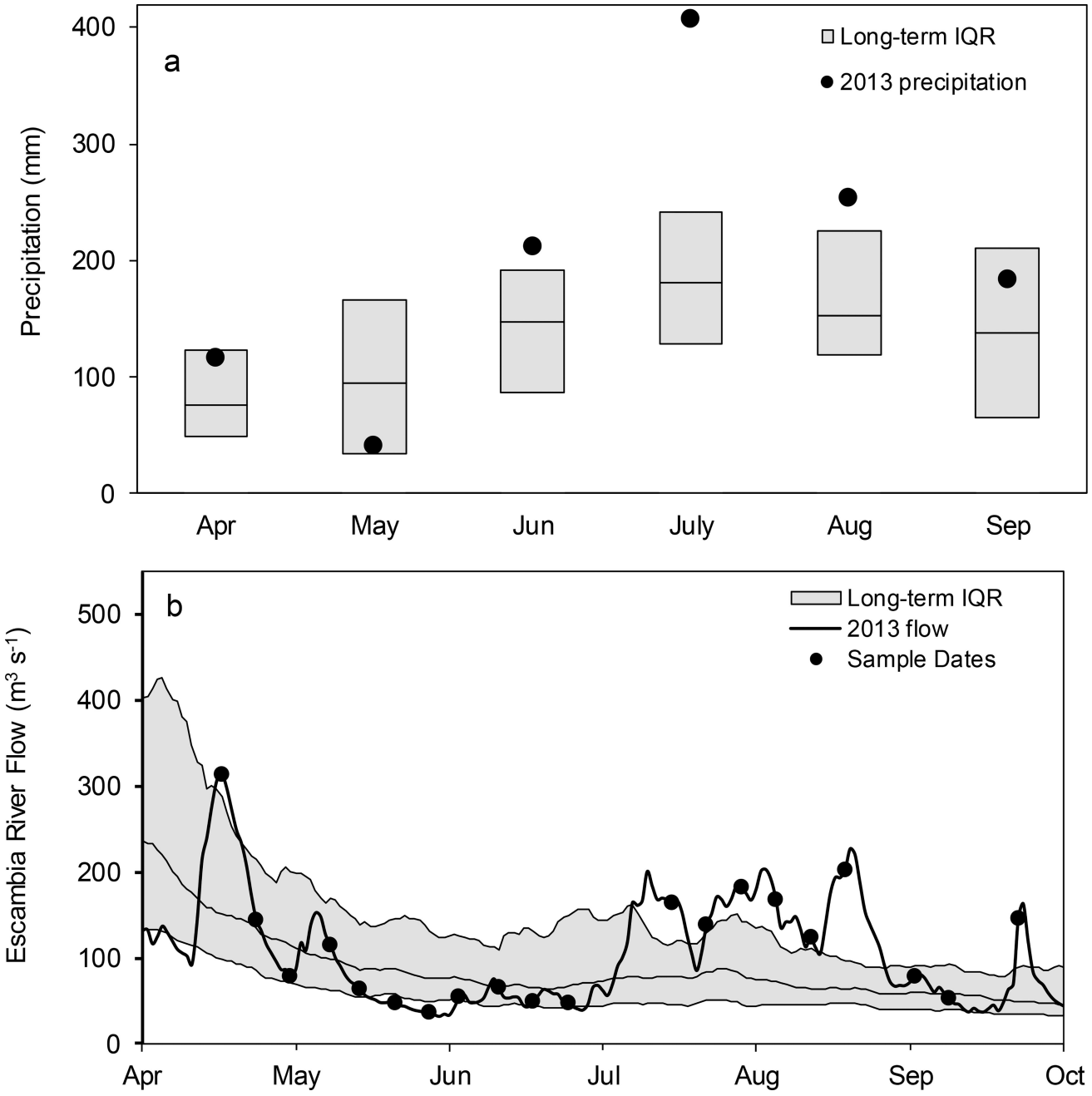

Figure 2.

A) Monthly precipitation (*symbols*) during 2013 superimposed on the 30-year (1980–2010) interquartile range (*shaded*) from Pensacola Regional Airport (station 13899, http://www.ncdc.noaa.gov). B) River discharge (*line*) from the Escambia River during 2013 superimposed on 30-year (1980–2010) interquartile ranges (*shaded*). Data from USGS gaging station 02375500 (http://waterdata.usgs.gove/nwis). Sample dates are indicated (*symbols*).

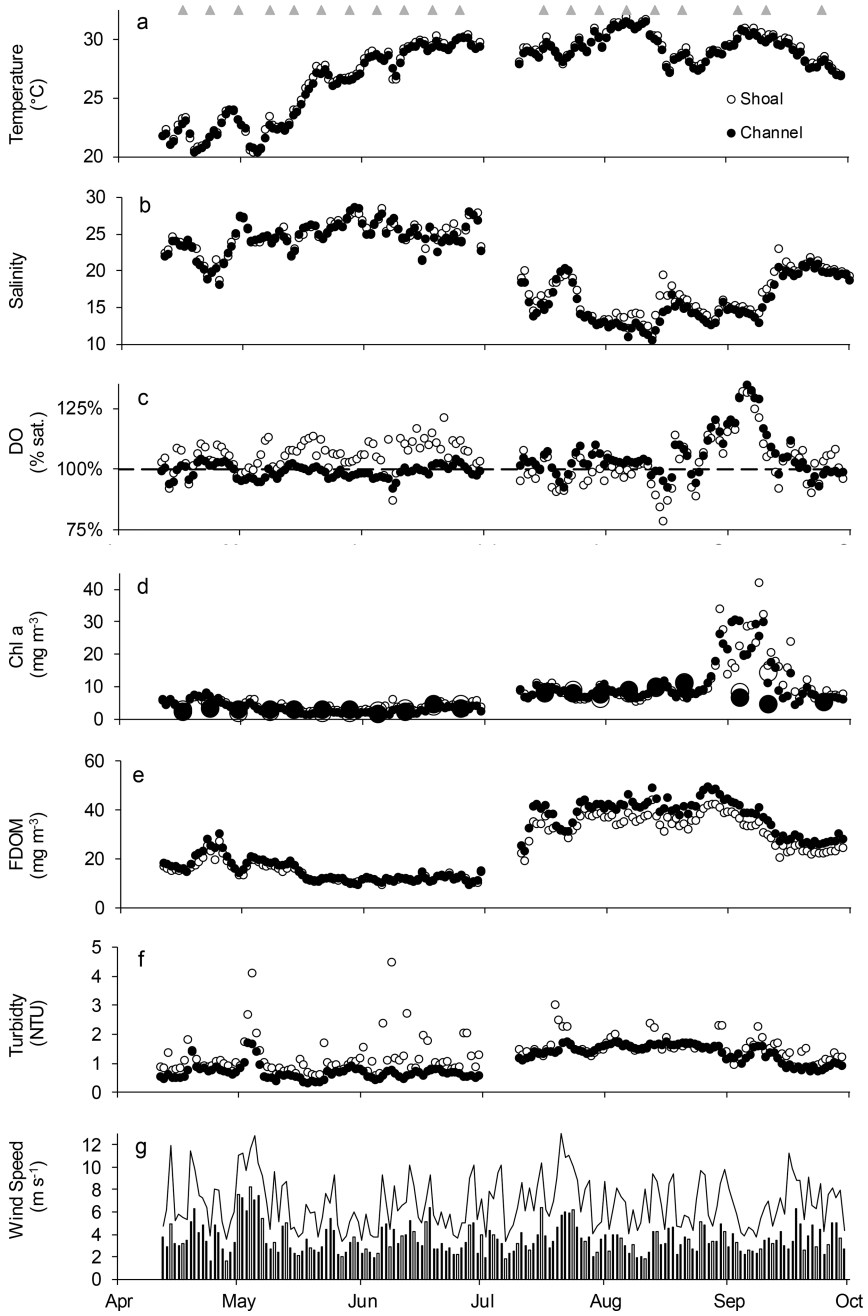

Figure 3.

Time series of daily average surface water variables at shoal (*open symbols*) and channel (*solid symbols*) sites: a) temperature (°C); b) salinity; c) dissolved oxygen (% saturation); d) calibrated Chl-*a* fluorescence and extracted Chl-*a* (*large circles*), both in units of mg m^{-3}; e) fluorescent dissolved organic matter (FDOM, mg m^{-3} of quinine sulfate dehydrate equivalents); f) turbidity (NTU); and g) daily mean (*vertical bars*) and maximum (*line segment*) wind speeds (m s^{-1}). The sampling dates are indicated in (a) as *shaded triangles*.

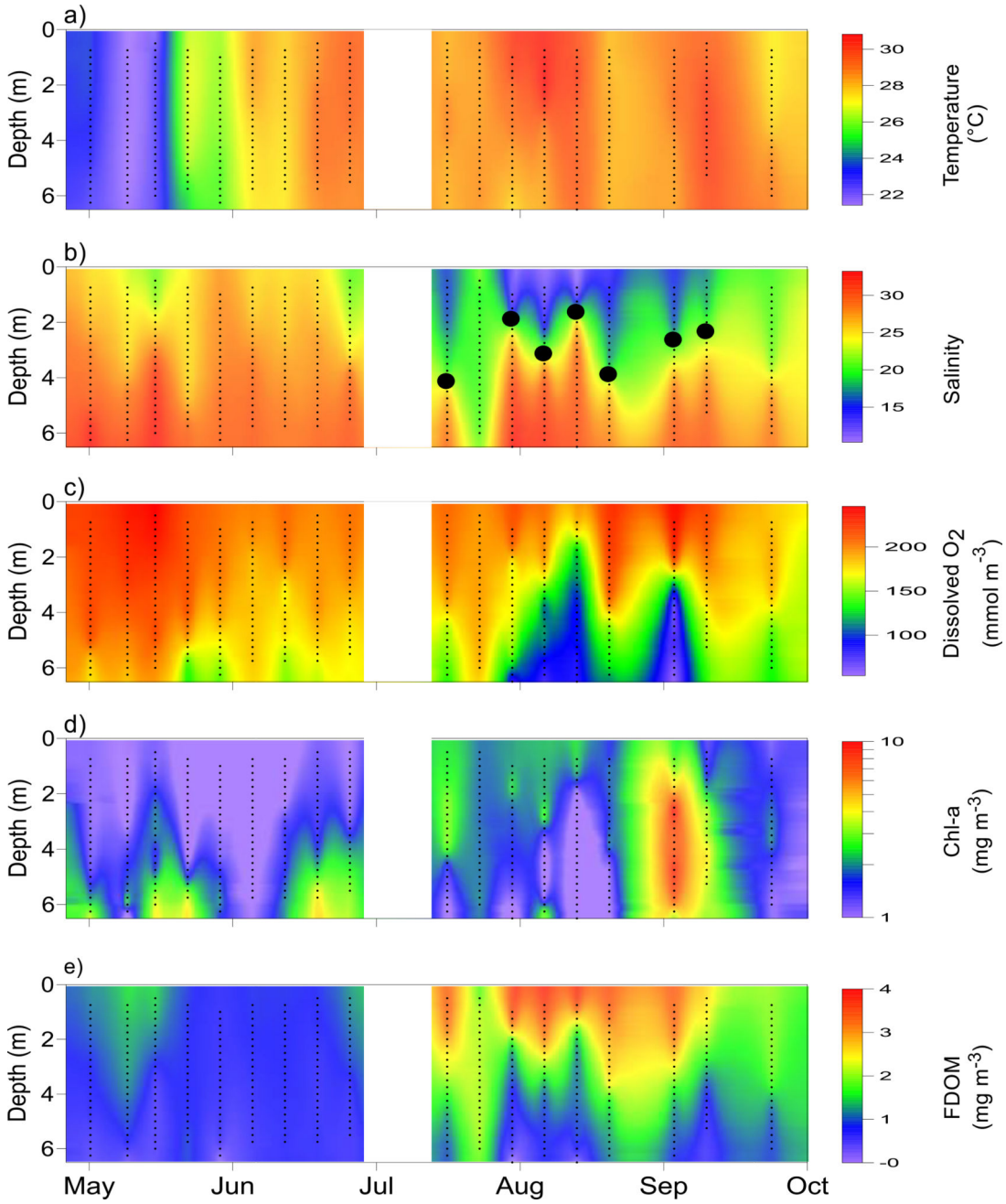

Figure 4.

Time series of vertical water column structure at the channel site interpolated from weekly to bi-weekly CTD profiles: a) temperature (°C), b) salinity, c) dissolved oxygen (mmol m $^{-3}$), d) Chl-*a* (mg m^{-3}), e) fluorescent dissolved organic matter (FDOM, mg m^{-3} of quinine sulfate dihydrate equivalents). The *small dots* indicate the position of the data used in the interpolations. The *large circles* in (b) indicate the location of the pycnocline when present. Interpolated values were calculated using the default kriging algorithm in Surfer® software.

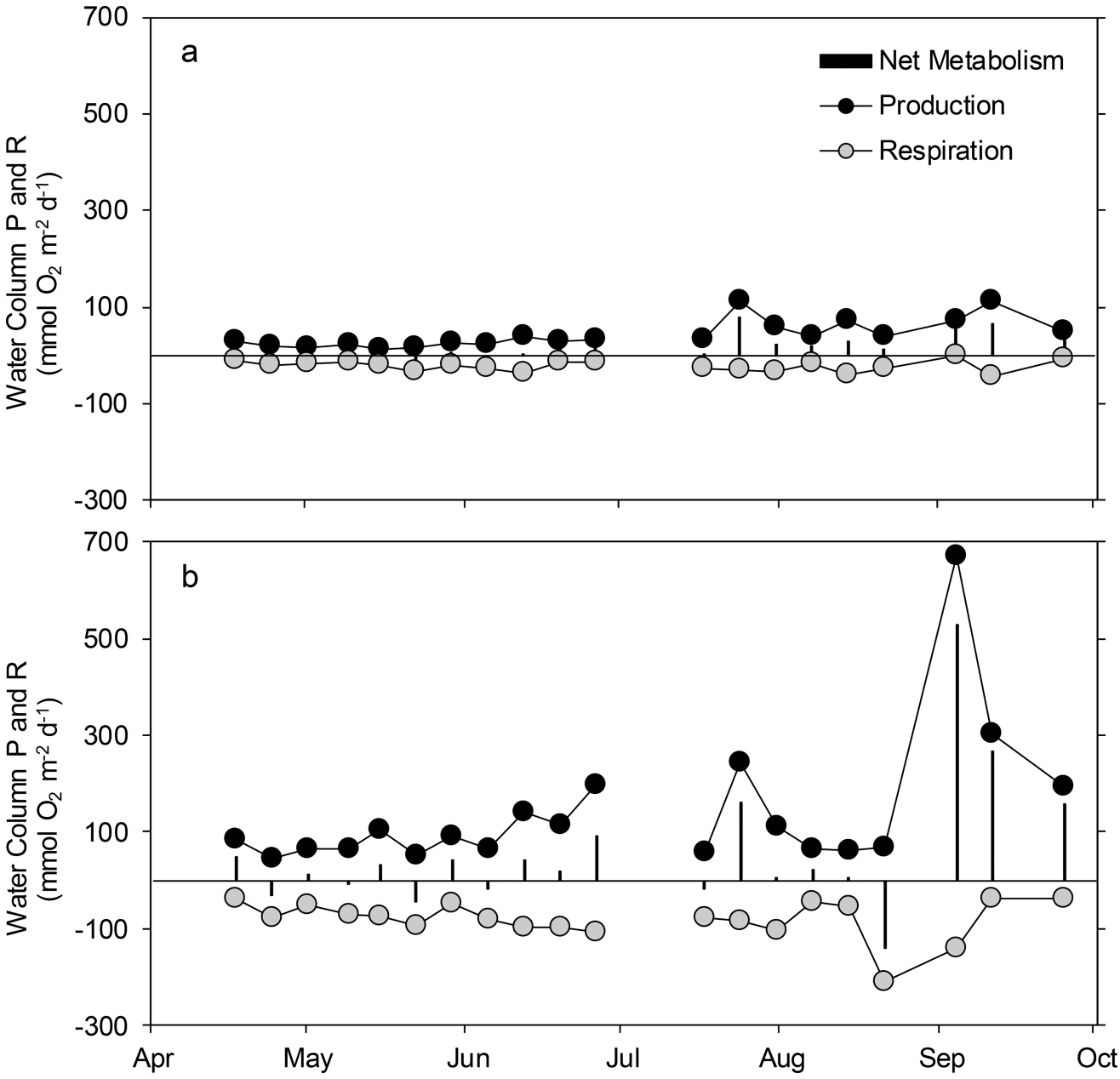

Figure 5.

Weekly time series of integrated plankton gross production (*solid symbols*), respiration (*shaded symbols*), and net metabolism (*drop lines*) at the shoal (a) and channel (b) sites. Respiration data were displayed as negative values for ease of graphing. Vertical scales are matched for comparison among sites.

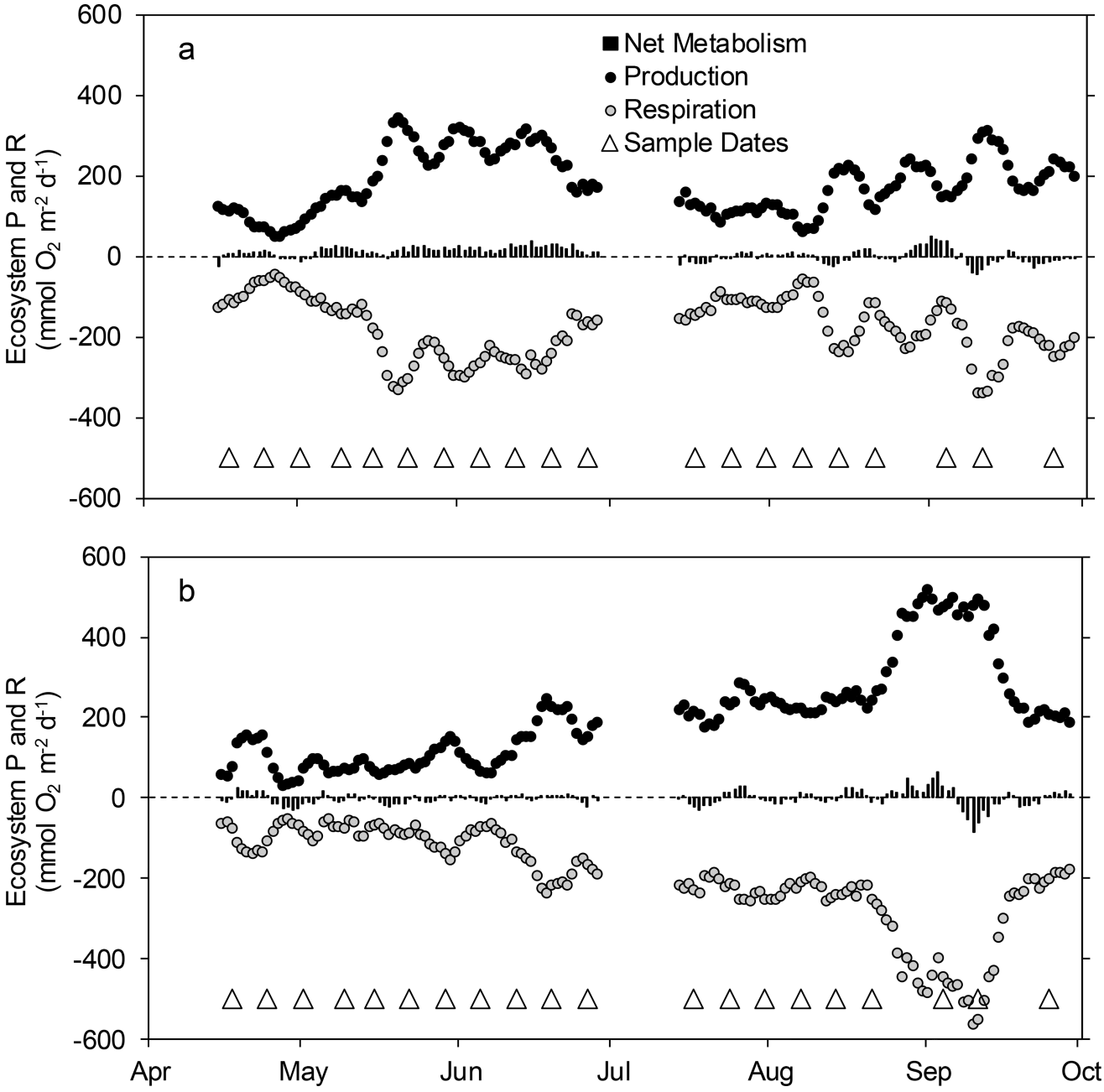

Figure 6.

Time series of daily ecosystem gross production (*solid symbols*), respiration (*shaded symbols*), and net metabolism (*drop lines*) calculated by the open water method at the shoal (a) and channel (b) sites. Values are 7-day moving window averages. The dates of bottle experiments are shown as *open triangles*.

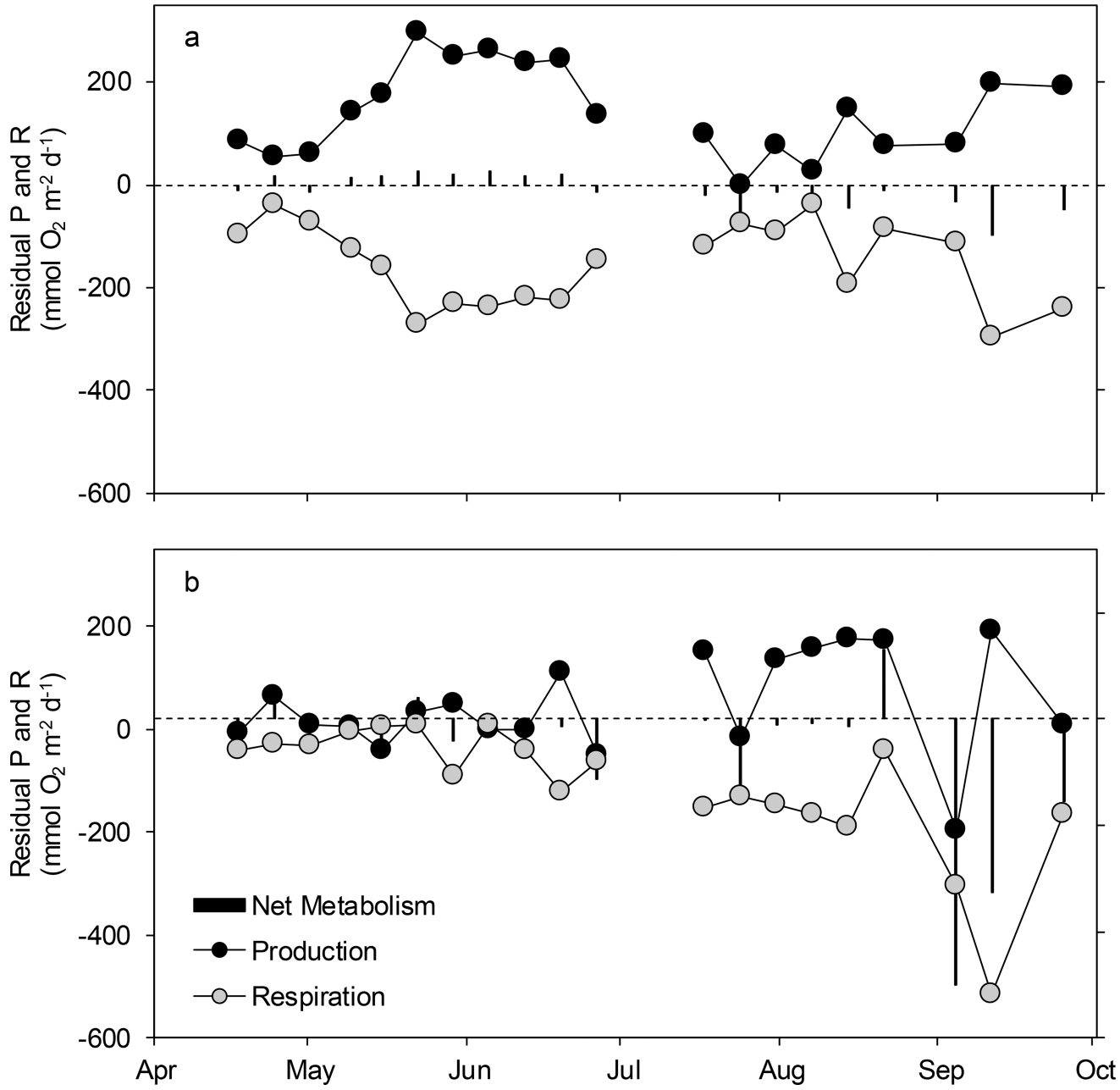

Figure 7.

Weekly time series of residual (ecosystem minus plankton) gross production (*solid symbols*), respiration (*shaded symbols*), and net metabolism (*drop lines*) at the shoal (a) and channel (b) sites. Respiration data are displayed as negative values for ease of graphing. Vertical scales are matched for comparison among sites.

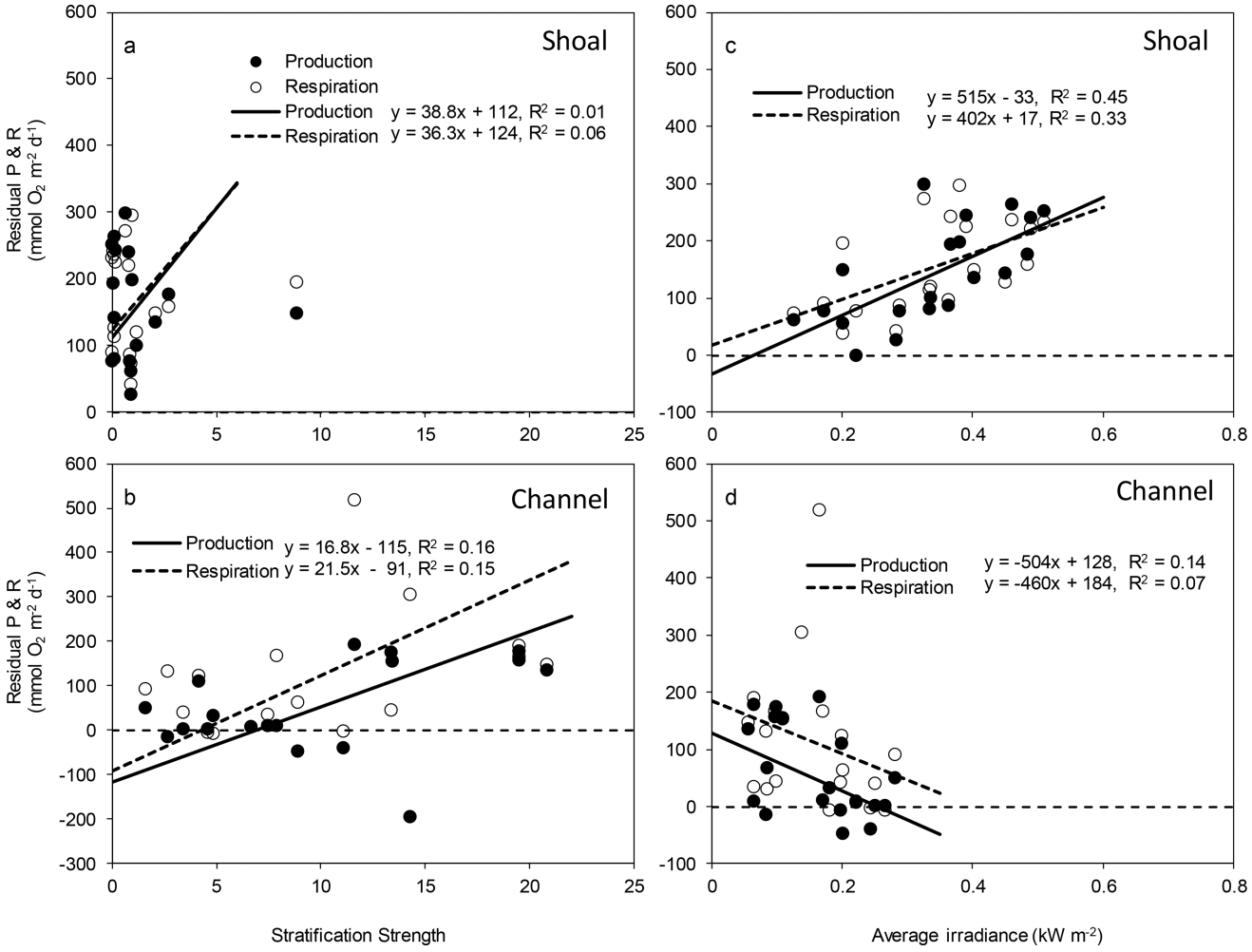

Figure 8.

Relationships between residual metabolism and key environmental variables, stratification strength, as surface-bottom delta salinity (a, b) and average water column irradiance (c, d), at the shoal (a, c), and channel (b, d) sites. Shown are residual gross production (*solid symbols*) and residual respiration (*open symbols*). The Model 2 reduced major axis regressions for residual production (*solid lines*) and residual respiration (*dashed lines*) are included as are the model equations.

Estuaries Coast. Author manuscript; available in PMC 2019 May 01.

Table 1

Medians and ranges of surface water quality variables based on weekly sampling at the shoal and channel sites for the spring (Apr.–Jun.) and summer (July–Sept) seasons. Included are temperature (°C), salinity, and dissolved O_2 (mmol m^{-3}) from CTD data. Nutrients (mmol m^{-3}) and Chl-*a* (mg m^{-3}) were measured from surface grab samples. The Chl-*a* normalized phytoplankton response variables were calculated from bottle experiments, including the initial slope of the PE curve (α^B: (mmol O_2 m^{-3} d^{-1})·(mg m^{-3} Chl a)$^{-1}$·(kW m^{-2})$^{-1}$)), the maximum photosynthetic rate (P_m^B: (mmol O_2 m^{-3} d^{-1}) (mg m^{-3} Chl a)$^{-1}$), and average water column irradiance (I_{avg}: kW m^{-2}). nd = Below detection (~0.4 μM) for NO_x.

	Shoal				Channel			
	Spring		Summer		Spring		Summer	
Temperature	26.8	*21.6–30.1*	30.1	*28.2–31.9*	26.5	*21.6–30.1*	29.8	*28.0–31.5*
Salinity	24.1	*19.7–27.5*	15.4	*12.0–20.4*	24.2	*19.6–28.0*	14.6	*10.8–19.7*
Dissolved O_2	237.2	*217.1–261.4*	223.7	*194.9–279.8*	216.0	*200.2–248.4*	233.1	*213.5–281.8*
NH_4	0.18	*0.13–0.69*	0.38	*0.18–1.39*	0.19	*0.08–0.34*	0.27	*0.22–1.03*
NO_X	nd	*nd-0.77*	nd	*nd-0.77*	nd	*nd*	nd	*nd*
PO_4	0.09	*0.07–0.16*	0.14	*0.12–0.50*	0.08	*0.06–0.13*	0.14	*0.12–0.20*
SiO_2	24.4	*6.9–33.1*	42.7	*29.2–67.0*	23.6	*8.0–37.6*	46.9	*35.5–64.2*
Chlorophyll a	3.0	*1.9–4.6*	8.3	*5.3–14.3*	2.8	*1.6–4.6*	8.0	*4.7–11.0*
α^B	4.3	*1.1–7.4*	8.3	*3.3–14.6*	4.8	*2.1–9.9*	8.7	*3.7–15.9*
P_m^B	0.44	*0.23–0.65*	0.42	*0.18–0.60*	0.38	*0.25–0.69*	0.36	*0.10–0.74*
I_{avg}	0.40	*0.13–0.51*	0.29	*0.17–0.38*	0.20	*0.07–0.28*	0.10	*0.06–0.17*

Table 2

Cross correlation analysis between channel and shoal sites of water quality time series during the spring (Apr-June) and summer (July-September) deployments. Shown are the maximum Pearson correlation coefficient (r) between the paired time series and the lag offset (30 minute time steps) at which the maximum correlation was observed. Negative lag scores indicated that the channel site lagged the shoal site, whereas positive lag scores indicate that the shoal site lagged the channel site.

	Spring		Summer	
Variable	***r***	***Lag***	***r***	***Lag***
Temperature	0.99	0	0.97	1
Salinity	0.89	1	0.88	−4
Dissolved oxygen	0.50	−5	0.73	−3
Turbidity	0.40	−7	0.35	5
Chlorophyll	0.76	0	0.55	5
FDOM	0.95	0	0.91	0

Table 3

Parameter estimates (SE) for a 2-way ANOVA of hourly volumetric daytime net production (P) and dark respiration (R) rates from bottle experiments (Incubation) and O_2 time series (Open Water) testing for site (Channel, Shoal) and season (Spring, Summer) effects, and their interactions. The intercept term refers to the mean P and R rates at the channel site in the spring. Other treatment means may be calculated by adding appropriate parameter estimates to the intercept. The coefficient of determination (R^2), the F-statistic, and number of observations (*n*) is included for each model.

	Incubation		Open Water	
	P	**R**	**P**	**R**
Intercept (Channel, Spring)	0.59	0.54**	0.57*	0.80**
	(0.30)	(0.09)	(0.22)	(0.26)
Site (Shoal)	0.06	0.05	3.52**	4.13**
	(0.42)	(0.13)	(0.32)	(0.37)
Season (Summer)	1.76**	0.08	1.16**	1.21**
	(0.44)	(0.14)	(0.31)	(0.37)
Site × Season	0.28	0.07	−1.30**	−1.61**
	(0.63)	(0.20)	(0.44)	(0.52)
R^2	0.51	0.06	0.36	0.35
F	12.55	0.74	60.6	57.2
n	40	40	328	328

* $p < 0.05$,

** $p < 0.01$

Table 4

Seasonal mean (± SE) water column (i.e., plankton), ecosystem, and residual (ecosystem minus water column) gross production, respiration, and net metabolism at shoal and channel sites during spring (April–June) and summer (July–September) seasons. Units are mmol O_2 m^{-2} d^{-1}. Also included are the average P:R ratios for each constituent. Note that mean P:R ratios were calculated from individual observations, thus do not match the ratio of the component means shown here.

	Shoal		Channel	
	Spring	**Summer**	**Spring**	**Summer**
Gross Production				
Water Column	23.9 ± *2.4*	64.4 ± *9.9*	93.4 ± *13.7*	197.4 ± *66.2*
Ecosystem	196.6 ± *13.3*	167.6 ± *10.7*	110.2 ± *10.1*	283.4 ± *16.5*
Residual	176.8 ± *26.2*	99.1 ± *22.9*	15.7 ± *13.9*	86.7 ± *43.2*
Respiration				
Water Column	21.1 ± *2.4*	26.6 ± *4.9*	76.5 ± *6.8*	87.9 ± *19.0*
Ecosystem	181.9 ± *13.3*	168.1 ± *12.2*	113.5 ± *9.4*	283.1 ± *16.9*
Residual	165.5 ± *23.1*	139.3 ± *28.3*	36.7 ± *12.6*	201.7 ± *45.4*
Net Metabolism				
Water Column	2.8 ± *3.1*	37.8 ± *9.2*	16.9 ± *12.0*	109.5 ± *66.0*
Ecosystem	11.5 ± *4.9*	−0.5 ± *5.3*	−3.3 ± *4.5*	0.3 ± *7.7*
Residual	11.3 ± *4.6*	−40.1 ± *10.3*	−20.9 ± *13.0*	−115.0 ± *64.7*
P:R Ratio				
Water Column	1.28 ± *0.19*	6.85 ± *4.37*	1.28 ± *0.17*	2.87 ± *0.89*
Ecosystem	**1.16** ± *0.05*	**1.10** ± *0.05*	**0.84** ± *0.30*	**0.97** ± *0.10*
Residual	1.07 ± *0.05*	0.68 ± *0.09*	0.92 ± *1.01*	0.83 ± *0.45*

Table 5

Pearson's correlation coefficients relating integrated metabolic and environmental variables at shoal and channel sites, including water column averages of temperature, salinity, Chl-*a*, water column irradiance (I_{avg}), and bottom-surface Δ salinity. Values in ***bold*** P <0.05. Values in ***bold underline*** P < 0.01.

	Shoal					Channel				
Gross Production	**Temp.**	**Salinity**	**Chl a**	**I_{avg}**	**Δ Salnity**	**Temp.**	**Salinity**	**Chl a**	**I_{avg}**	**Δ Salnity**
Water Column	**0.61**	**−0.55**	**0.55**	−0.26	0.23	0.34	−0.19	**0.92**	−0.02	0.08
Ecosystem	0.30	0.44	0.01	**0.61**	−0.02	**0.65**	−0.36	**0.76**	−0.33	0.42
Residual	0.12	**0.62**	−0.17	**0.67**	−0.09	0.30	−0.16	0.37	−0.38	0.40
Respiration										
Water Column	0.35	−0.24	0.01	−0.18	0.39	0.23	−0.24	0.30	−0.14	0.10
Ecosystem	0.34	0.36	0.08	**0.52**	0.08	**0.64**	−0.34	**0.70**	−0.31	0.42
Residual	0.30	0.42	0.09	**0.57**	0.02	**0.57**	−0.26	**0.60**	−0.27	0.38
Net Metabolism										
Water Column	**0.48**	**−0.46**	**0.60**	−0.20	0.05	0.29	−0.13	**0.86**	0.02	0.05
Ecosystem	−0.18	0.37	−0.37	0.43	−0.41	−0.12	−0.07	0.21	−0.04	−0.07
Residual	−0.44	**0.54**	**−0.64**	0.37	−0.27	−0.30	0.12	**−0.84**	−0.02	−0.06

Estuaries Coast. Author manuscript; available in PMC 2019 May 01.

Table 6

Alternative estimates of components of ecosystem production and respiration (mmol O_2 m^{-2} d^{-1}) at the channel site for the seven dates when water column stratification was observed (see Fig. 4). Estimates of surface layer, lower layer, and benthic components were calculated as described in the text, and their sum was compared to estimates from the open water method.

Gross Production						
Date	***Pycnocline (m)***	***Surface Layer***	***Lower Layer***	***Benthos***	***Total Components***	***Total Open Water***
7/17	4.1	147.9	3.9	0.4	152.2	211.6
7/31	1.9	78.4	24.0	0.4	102.7	246.5
8/7	3.1	117.5	1.1	0.3	118.9	221.7
8/14	1.6	65.1	3.6	0.2	68.9	236.5
8/21	3.9	158.7	4.4	0.4	163.5	241.6
9/4	2.6	210.8	195.9	1.6	408.3	473.7
9/11	2.3	194.3	260.1	2.2	456.7	493.1
Average	2.8	138.9	70.4	0.8	210.2	303.5
Respiration						
Date	*Pycnocline (m)*	*Surface Layer*	*Lower Layer*	*Benthos*	*Total Components*	*Total Open Water*
7/17	4.1	162.1	23.5	11.3	196.9	231.9
7/31	1.9	80.1	71.8	11.3	163.2	252.0
8/7	3.1	110.9	21.0	11.3	143.2	209.4
8/14	1.6	67.2	40.1	11.3	118.5	243.9
8/21	3.9	165.5	71.8	11.3	248.6	251.9
9/4	2.6	198.0	78.1	11.3	287.4	445.0
9/11	2.3	218.2	22.1	11.3	251.6	553.8
Average	2.8	143.1	46.9	11.3	201.4	312.6